

Soliton-sound interactions in quasi-one-dimensional Bose-Einstein condensates

N.G. Parker, N.P. Proukakis, M. Leadbeater, and C.S. Adams

Department of Physics, University of Durham, South Road, Durham DH1 3LE, United Kingdom

Longitudinal confinement of dark solitons in quasi-one-dimensional Bose-Einstein condensates leads to sound emission and reabsorption. We perform quantitative studies of the dynamics of a soliton oscillating in a tight dimple trap, embedded in a weaker harmonic trap. The dimple depth provides a sensitive handle to control the soliton-sound interaction. In the limit of no reabsorption, the power radiated is found to be proportional to the soliton acceleration squared. An experiment is proposed to detect sound emission as a change in amplitude and frequency of soliton oscillations.

PACS numbers: 03.75.Lm, 42.65.Tg

The experimental realisation of dilute atomic Bose-Einstein condensates (BEC) [1] has introduced an unparalleled platform from which to study the dynamical behaviour of nonlinear systems. Of great interest is the stability of topological structures, such as vortices and dark solitary waves. Recent experiments at low temperatures have highlighted the temperature-independent crystallization [2] and decay [3] of vortex structures. Related theoretical work has indicated the importance of vortex-sound interactions [4]. Following the recent experimental observation of dark solitary waves (henceforth referred to as dark solitons) in BEC's [5], one can now study the coupling of solitons to the background sound field.

Dark solitons are robust localised one-dimensional defects characterised by a notch in the ambient condensate density and a phase slip across the centre. They are supported in repulsive (defocussing) nonlinear media where the kinetic dispersion of the wave is balanced by the nonlinear interaction. In three-dimensional geometries they are prone to decay into lower energy topological structures such as vortex rings [6]. However, in quasi-one-dimensional (quasi-1D) geometries, where the transverse condensate size is of the order of the healing length, solitons are expected to exhibit longer lifetimes, due to the suppression of transverse excitations [7].

In the context of nonlinear optics [8], dark solitons on a homogeneous background can become intrinsically unstable to modifications of the nonlinearity within the optical medium (e.g. due to saturation effects) [9]. In quasi-1D BEC's, modified nonlinearities can arise from the transverse dimensions that have been integrated out, as considered for longitudinally homogeneous condensates in [10]. The longitudinal confinement of current atomic BEC experiments leads to an additional mechanism by which the integrability of the system can be broken [11, 12, 13]. In this paper we perform detailed quantitative analysis of the stability of dark solitons in quasi-1D geometries under longitudinal confinement, and find that dissipation due to the longitudinal inhomogeneity dominates over decay arising from coupling to transverse modes [10]. Our axial configuration consists of a tight dimple trap (where the soliton resides) embedded in a weaker harmonic potential. Such a geometry en-

ables us to control and examine the interplay between sound emission and reabsorption by the oscillating soliton. In the limit of no reabsorption, the rate of emission is found to be proportional to the local soliton acceleration squared, as predicted for optical solitons in *homogeneous* nonlinear waveguides [9]. Finally we propose a controllable experiment where the soliton-sound interactions can be quantified by measuring the amplitude and frequency of the soliton oscillations.

Our analysis is based on numerical simulations of the Gross-Pitaevskii Equation (GPE), describing the dynamics of weakly-interacting BEC's in the limit of low temperature,

$$i\hbar \frac{\partial \psi}{\partial t} = -\frac{\hbar^2}{2m} \nabla^2 \psi + V_{\text{ext}} \psi + g|\psi|^2 \psi. \quad (1)$$

Here ψ is the order parameter of the system, V_{ext} the confining potential, m the atomic mass and $g = 4\pi\hbar^2 a/m$ the scattering amplitude, where a is the s -wave scattering length. In the limit of tight transverse confinement, the condensate dynamics are effectively longitudinal [14]. By integrating out the transverse degrees of freedom, the GPE reduces to a one-dimensional (1D) form with a modified coupling coefficient $g_{1D} = g/(2\pi l_{\perp}^2)$, where $l_{\perp} = \sqrt{\hbar/m\omega_{\perp}}$ is the transverse harmonic oscillator length and ω_{\perp} the transverse trapping frequency. On a homogeneous background density n_{1D} , a dark soliton of speed v and position, $z' = (z - vt)$, is defined as,

$$\psi(z, t) = \sqrt{n_{1D}} [\beta \tanh(\beta z'/\xi) + i(v/c)] e^{-i\mu_{1D} t/\hbar} \quad (2)$$

where $\mu_{1D} = g_{1D} n_{1D}$ is the one-dimensional chemical potential, $c = \sqrt{\mu_{1D}/m}$ the Bogoliubov speed of sound, $\beta = \sqrt{1 - (v/c)^2}$, and $\xi = \hbar/\sqrt{m\mu_{1D}}$ is the healing length characterising the size of the soliton.

We consider a trap of the form

$$V_{\text{ext}} = \begin{cases} \frac{1}{2}m\omega_z^2 z^2 & \text{for } |z| \leq z_0 \\ V_0 + \frac{1}{2}m\omega_{\zeta}^2 (|z| - z_0)^2 & \text{for } |z| > z_0 \end{cases} \quad (3)$$

where we have defined the 'cut-off' depth of the inner 'dimple' trap as $V_0 = \frac{1}{2}m\omega_z^2 z_0^2$ (see Fig. 1). Sound waves generated by the oscillating soliton can either be trapped within the dimple or escape to the outer trap, depending on the value of the cut-off V_0 relative to the chemical

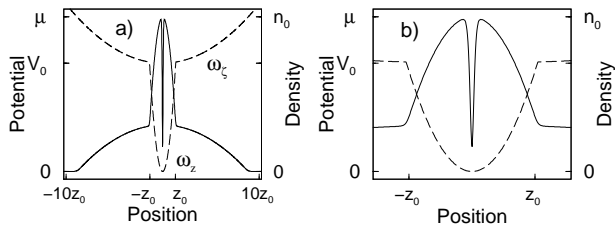


FIG. 1: (a) Initial longitudinal condensate density (solid line) for a double trap geometry (dashed line) with a soliton centred at the origin. (b) Enlarged image of central region.

potential μ_{1D} . For a sufficiently weak outer trap, the density in the outer region and close to the dimple becomes approximately homogeneous (Fig. 1(b)), and as a first approximation we initially solve the 1D GPE in the limit $\omega_\zeta = 0$. We shall return to the experimentally relevant case of $\omega_\zeta \neq 0$ and 3D simulations later. The effect of the emitted sound on soliton dynamics can be determined by monitoring the ‘soliton energy’ [15], a quantity determined by integrating the functional,

$$\varepsilon(\psi) = \frac{\hbar^2}{2m} |\nabla\psi|^2 + V_{\text{ext}} |\psi|^2 + \frac{g}{2} |\psi|^4, \quad (4)$$

across the soliton region ($z_s \pm 5\xi$) and subtracting the corresponding contribution of the background fluid.

Fig. 2 shows the temporal evolution of the soliton energy for different cut-offs (corresponding to different amounts of sound reabsorption), all of which display a periodicity of approximately $\omega_z/\sqrt{2}$ due to the motion of the soliton in the trap [11, 12, 13]. One can discriminate two limiting cases: (i) For sufficiently high cut-offs (here $V_0 \geq 1.2\mu_{1D}$) all emitted sound becomes trapped in the dimple, leading principally to the excitation of the dipole mode [11]. The combined effect of the dipole mode and soliton, oscillating at different frequencies, induces beating of characteristic period $\tau \approx 22$ (see Fig. 2). (ii) For low cut-offs ($V_0 \leq 0.4\mu_{1D}$) there is essentially pure emission (no reabsorption) of sound by the soliton. This behaviour is consistent with the change in energy experienced by a classical particle of negative mass oscillating in a harmonic trap, subject to a dissipative force which induces an energy loss proportional to the acceleration squared [16]. The observation that the soliton dynamics changes significantly around $V_0 \approx \mu_{1D}$ (since sound excitations have energy of the order of the chemical potential) provides a sensitive handle on the soliton-sound interaction, which can be controlled experimentally.

The dissipative dynamics of a dark soliton in a shallow dimple trap are investigated in Fig. 3. As the soliton oscillates, it becomes asymmetrically deformed [16] and tries to adjust to the inhomogeneous background by radiating counter-propagating sound pulses (Fig. 3(a)). Fig. 3(b) shows the power emitted by the soliton as a function of time. At the bottom of the trap there is no sound emission since Eq. (2) becomes the local so-

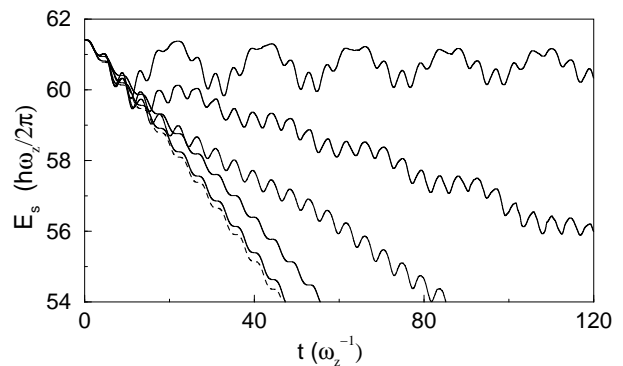


FIG. 2: Soliton energy versus time for a soliton of initial speed $0.5c$ and position $z = 0$ in a relatively weak inner harmonic trap ($\mu_{1D} = 70\hbar\omega_z$) for various potential cutoffs V_0 (from top to bottom): $1.1\mu_{1D}$, $1.02\mu_{1D}$, $1\mu_{1D}$, $0.8\mu_{1D}$ and $0.4\mu_{1D}$. The lowermost dotted line corresponds to the theoretical prediction of Eq. (5), valid in the limit of no reabsorption.

lution to the GPE, while at the zenith of the first few oscillations, the soliton radiates maximum power. This sound emission (which modifies the soliton depth) leads to an increase in the soliton speed and amplitude of oscillations, which in turn causes a gradual increase in the peak power radiated. As the soliton approaches the edge of the dimple, it experiences a smoothing of the effective potential due to fluid healing. This reduces the emission at the trap edge, as manifested in the ‘intermediate’ dips at $\omega_z t \approx 25$ and 29.5 . Eventually at $\omega_z t \approx 35$ the soliton escapes the trap [11].

In the context of nonlinear optics, multiscale asymptotic techniques predict that an unstable optical soliton, propagating in a homogeneous nonlinear waveguide, emits sound at a rate proportional to the soliton acceleration squared [9], such that,

$$\frac{dE_s}{dt} = -\frac{c}{c^2 - v^2} \left[\frac{2c^2}{n} \left(\frac{\partial N_s}{\partial v} \right)^2 + 2v \left(\frac{\partial N_s}{\partial v} \right) \left(\frac{\partial S_s}{\partial v} \right) + \frac{n}{2} \left(\frac{\partial S_s}{\partial v} \right)^2 \right] \left(\frac{dv}{dt} \right)^2. \quad (5)$$

Here n is the local background density, S_s the total phase slip across the moving soliton, and $N_s = \int (n - |\psi|^2) dz$ the number of particles displaced by the soliton. In the optical case, the breakdown of integrability leading to sound emission arises from modifications in the nonlinearity within the medium, as opposed to the longitudinal confinement discussed above. It may therefore come as a surprise that this expression could also be applicable to the inhomogeneous case. In fact, this can only be valid in double trap structures of Eq. (3) if the dimple trap is sufficiently shallow that it essentially allows complete escape of sound to the outer trap; even then, this result will only hold until the emitted sound returns to the dimple region after reflection from the outer trap. In this limit, the asymptotic conditions become practically indis-

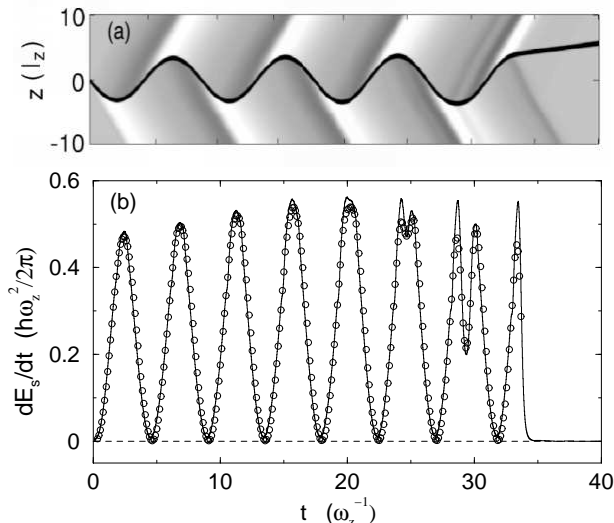


FIG. 3: (a) Space-time plot of a soliton oscillating in a dimple trap with $V_0 = 0.4\mu_{1D}$ where $\mu_{1D} = 35\hbar\omega_z$. Deviations from background density correspond to sound (light/dark regions indicate high/low densities), with the sound amplitude roughly 2% of the background. (b) Power emitted by the soliton as calculated from the energy functional (solid line), compared with the prediction of Eq. (5) (circles).

tinguishable from the homogeneous ones, thus justifying the above approach. The validity of Eq. (5) is not dependent on the origin of the instability, but rather on the fact that the emitted sound escapes from the soliton region. Note that the effect of the dimple confinement is implicit in the variations of the parameters S_s , c and n , and, contrary to the homogeneous case [9], this result will hold for *all* soliton speeds, due to the continuously-induced ‘soliton instability’ caused by the longitudinal confinement. Fig. 3(b) confirms the applicability of Eqs. (5) (circles) in the limit $V_0 \ll \mu_{1D}$ by direct comparison to the 1D GPE simulations (solid line). Further evidence is provided in Fig. 2 which shows clearly that as the cut-off is decreased, the variation of energy with time (solid lines) approaches the above analytical result in the limit of no reabsorption (dotted line). We stress that Eq. (5) will *not* hold in the usual infinite harmonic traps, where multiscale asymptotic technique must be combined with boundary layer theory [11].

Simulations of the 3D GPE with cylindrical symmetry (still under the assumption of a homogeneous outer trap) confirm the qualitative findings of Fig. 2. In particular, in the limit $\mu_{3D}/\hbar\omega_\perp \approx 1.2$ (where the soliton was recently predicted to be stable against transverse decay [10]) we find the dominant decay mechanism to be due to *axial* inhomogeneity. The coupling to transverse modes [13] merely leads to an additional *oscillation* of the soliton energy in time (Fig. 4), whose amplitude increases as the transverse confinement is relaxed [17]. Subtracting the average oscillation in the 3D longitudinal energy (Fig. 4(b)) from the energy of the soliton region gives es-

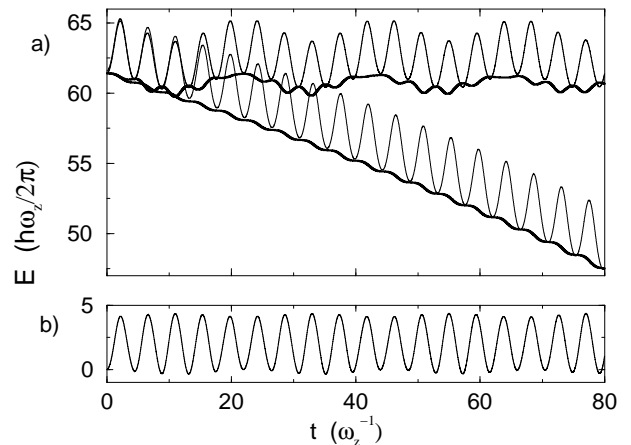


FIG. 4: (a) Soliton energies obtained from the 3D GPE (thin lines) vs. corresponding 1D GPE results (thick lines) for cut-offs of $V_0 = 1.1\mu_{1D}$ (top) and $V_0 = 0.4\mu_{1D}$ (bottom). The longitudinal parameters are as in Fig. 2, and trap aspect ratio is set to $\omega_\perp/\omega_z \approx 250$, such that the initial density profile in the z -direction is identical to the one-dimensional density. (b) The oscillation in the total longitudinal energy due to the coupling to transverse modes, as measured by integrating the energy functional longitudinally.

entially perfect agreement with the 1D results (Fig. 2).

Finally we extend our earlier treatment to the experimentally relevant case of $\omega_\zeta \neq 0$. We consider a BEC in a quasi-1D geometry [18] in a cylindrically symmetric trap with frequencies ω_ζ (longitudinal) and ω_\perp (transverse), and then add an inner dimple potential (ω_z), such that the longitudinal confinement is as shown in Fig. 1. This could be realized, for example, by a dimple microtrap created optically within a larger magnetic trap. The key points for such a realization are: (i) a very weak longitudinal trap frequency ω_ζ , such that the sound escaping from the inner trap is not reflected back from the outer trap within the timescale of interest, and (ii) a sufficiently tight inner trap ω_z such that the oscillating soliton emits sound at a rate fast enough that its amplitude increases noticeably before other decay mechanisms become important.

Experimentally, the effect of soliton-sound interactions can be probed by determining the soliton path via repeated time of flight measurements, and comparing paths for different depths of the dimple trap. The best signature for this effect arises when comparing the case of an effectively infinite cut-off to that of a lower cut-off, which nonetheless permits a sufficient number of soliton oscillations. Since the soliton rapidly escapes the trap for $V_0 < \mu_{1D}$, we thus propose the use of $V_0 = \mu_{1D}$ as a low cut-off, for which the soliton remains confined and ultimately decays to a sound pulse. Such a comparison has been performed for the double-trap system in Fig. 5, for both harmonic and gaussian dimple traps. One clearly observes a change in both amplitude and frequency of the soliton oscillations as a result of sound emission. These

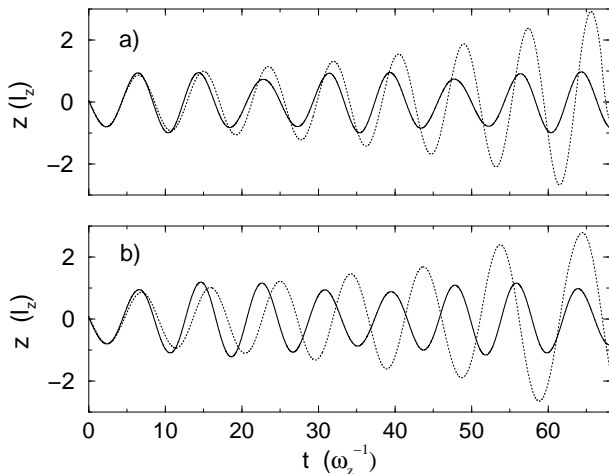


FIG. 5: Soliton path in a longitudinal double-trap configuration for (a) tight harmonic inner trap and (b) gaussian dimple $V_0[1 - \exp(-\alpha z^2)]$. Each graph shows the cases of a cut-off $V_0 = \mu_{1D}$ (dotted line) compared to an effectively infinite cut-off $V_0 = 5\mu_{1D}$ (solid line), for a soliton with initial speed $0.2c$. The gaussian dimple in (b) is chosen such that it yields same initial oscillation frequencies as the harmonic dimple (achieved for $\alpha = \omega_z^2/2V_0$). The outer trap is harmonic in both cases, with relatively weak confinement $\omega_\zeta = \omega_z/10$.

effects become more noticeable in the gaussian trap, for

which the required cut-off for total sound entrapment is larger than the harmonic one. Choosing ‘typical’ parameters $\omega_\zeta = 2\pi \times 5$ Hz, $\omega_z = 10\omega_\zeta$ and $\omega_\perp = 250\omega_\zeta$ and $\mu_{3D} = 8\hbar\bar{\omega}$ where $\bar{\omega} = (\omega_\zeta\omega_\perp^2)^{1/3}$, we find respectively for a ^{23}Na (^{87}Rb) condensate, a one-dimensional peak dimple density of $n_{1D} = 5 \times 10^7$ (1.5×10^7) m^{-1} , condensate atom number $N = 18,000$ (3,500) and a total observation timescale for Fig. 5 of $\tau_{\text{exp}} = 220$ ms, consistent with the expected soliton lifetime in such systems [10, 11, 12].

In summary, we have performed quantitative studies of the dynamics of dark solitons oscillating in trapped quasi-one-dimensional Bose condensates under longitudinal double-trap confinement. This geometry is ideal for controlling the interplay between sound emission and reabsorption, and we have identified two limiting cases: (i) In the limit of no reabsorption, the power emitted by the soliton is proportional to the square of its acceleration. (ii) The opposite limit of effectively infinite traps (such as harmonic traps in which soliton experiments have been performed) leads to the anticipated stabilization against soliton decay. We suggest that the sound radiation can be quantified by tracking the position of the dark soliton in suitably engineered traps, which allow for precise control of the soliton-sound interaction.

We acknowledge discussions with C. Barenghi, K. Burnett, W.D. Phillips and G.V. Shlyapnikov. Funding was provided by UK EPSRC.

-
- [1] M. Inguscio, S. Stringari, and C. Wieman, Eds. *Bose-Einstein Condensation in Atomic Gases* (IOS Press, Amsterdam, 1999).
- [2] J. R. Abo-Shaeer, C. Raman, and W. Ketterle, *Phys. Rev. Lett.* **88**, 070409 (2002).
- [3] S. I. Davis, P. C. Hendry, and P. V. E. McClintock, *Physica B* **280**, 43 (2000).
- [4] W. F. Vinen, *Phys. Rev. B* **61**, 1410 (2000); M. Leadbeater, T. Winiecki, D. C. Samuels, C. F. Barenghi, and C. S. Adams, *Phys. Rev. Lett.* **86**, 1410 (2001); M. Leadbeater, D. C. Samuels, C. F. Barenghi, and C. S. Adams, *Phys. Rev. A* **67**, 015601 (2003).
- [5] S. Burger *et al.*, *Phys. Rev. Lett.* **83**, 5198 (1999); J. Denschlag *et al.*, *Science* **287**, 97 (2000); Z. Dutton, M. Budde, C. Slowe, and L. V. Hau, *Science* **293**, 663 (2001).
- [6] B. P. Anderson *et al.*, *Phys. Rev. Lett.* **86**, 2926 (2001); D. L. Feder, M. S. Pindzola, L. A. Collins, B. I. Schneider, and C. W. Clark, *Phys. Rev. A* **62**, 053606 (2000); J. Brand and W. P. Reinhardt, *Phys. Rev. A* **65**, 043612 (2002); S. Komineas and N. Papanicolaou, *Phys. Rev. Lett.* **89**, 070402 (2002).
- [7] A. E. Muryshev, H. B. van Linden van den Heuvell, and G. V. Shlyapnikov, *Phys. Rev. A* **60**, R2665 (1999).
- [8] Y. S. Kivshar and B. Luther-Davies, *Phys. Rep.* **278**, 81-197 (1998).
- [9] D. E. Pelinovsky, Y. S. Kivshar, and V. V. Afanasjev, *Phys. Rev. E* **54**, 2015 (1996).
- [10] A. E. Muryshev, G. V. Shlyapnikov, W. Ertmer, K. Senegstock, and M. Lewenstein, *Phys. Rev. Lett.* **89**, 110401 (2002).
- [11] T. Busch and J. R. Anglin, *Phys. Rev. Lett.* **84**, 2298 (1999); see also cond-mat/9809408 (1998).
- [12] P. O. Fedichev, A. E. Muryshev, and G. V. Shlyapnikov, *Phys. Rev. A* **60**, 3220 (1999).
- [13] G. Huang, J. Szeftel, and S. Zhu, *Phys. Rev. A* **65**, 053605 (2002).
- [14] A. D. Jackson, G. M. Kavoulakis, and C. J. Pethick, *Phys. Rev. A* **58**, 2417 (1998).
- [15] This procedure cannot discriminate between soliton and sound energy present in the interval; however, this sound contribution is much smaller than the soliton energy.
- [16] N. G. Parker, N. P. Proukakis, M. Leadbeater, and C. S. Adams, cond-mat/0304148 (2003).
- [17] By solving the 3D GPE in the longitudinally homogeneous limit ($\omega_z = \omega_\zeta = 0$), we have investigated whether the coupling to transverse modes leads to soliton decay [10] within the timescale probed in this paper. We find no *dissipation* arising when $\mu_{3D}/\hbar\omega_\perp < 10$, and already observe decay via the snake instability at $\mu_{3D}/\hbar\omega_\perp \approx 18$.
- [18] A. Görlitz *et al.*, *Phys. Rev. Lett.* **87**, 130402 (2001).